

Three-band model of high- T_c superconductivity

D. C. Mattis

Department of Physics, University of Utah, Salt Lake City, Utah 84112

(Received 15 September 1998)

We reduce the three-band model of planar CuO_2 to a single-band of *composite* fermions. We obtain hopping parameters $t_{\text{eff}}(R_{ij})$, repulsive potentials U_{eff} and $V(R_{ij})$, and the superexchange interactions $J(R_{ij})$ necessary for both antiferromagnetism and superconductivity. The ratios of these quantities are determined by a unique parameter $x \approx 3.9t_{pd}/U_{dd}$. Pairing symmetry crosses over from “extended s ” to “ d ” as function of carrier concentration. We show why only the latter survives near the antiferromagnetic point.

[S0163-1829(99)00110-1]

INTRODUCTION

In earlier studies we reduced the three-band “limit model” of copper-oxide planes to a one-band model in which *composite* charged particles interacted solely through a hard-core zero-range repulsion.¹ The limit in question consists of taking $t_{pd}/U_{dd} \rightarrow 0$ while keeping $t_{pd}^2/2U_{dd} \equiv t^*$, the unit of energy, finite. The present theory is for nonzero values of t_{pd}/U_{dd} and it is far more compelling. Among other results possible to obtain at finite values of t_{pd}/U_{dd} , we arrive at a reliable formula for the strength of the superexchange interaction—at present the leading candidate mechanism for high- T_c superconductivity. We also determine that for t_{pd}/U_{dd} approaching or exceeding 0.5, what was formerly the hard-core repulsion U_{eff} may become quite “squishy” or even soft.

We exhibit the eigenstates and the self-energies of the charged composite particles and their effective hopping parameter $t_{\text{eff}}(R_{ij})$. We find also that they repel via a weak two-body scalar interaction potential $V(R_{ij})$ and the finite zero-range interaction U_{eff} . Our calculated superexchange interaction $J(R_{ij})$ is of the right sign and magnitude to promote both antiferromagnetism and high- T_c superconductivity. We arrive at these conclusions using orthogonal orbitals, identifying the *low-lying states* of a three-band model of electrons with those of a one-band model of interacting, composite, charge carriers.² The interactions affecting these entities are obtained in a Born-Oppenheimer-type scheme in lowest order of perturbation theory, but when the errors are estimated they are found acceptably small.

Already in Ref. 1 the calculated energies were found to be naturally expressible as multiples of the unit of energy, t^* . An additional feature is that their ratios are uniquely determined by a second parameter defined as $x \equiv 2t_{pd}T(0)/U_{dd}$ [with $T(0) \approx 1.9$ given in Table I] which we now take to be nonzero.³ Aside from the scale of energy determined by t^* , x is the sole adjustable parameter with which to fit all known features of the microscopic model to the actual materials. Nevertheless there does remain a meaningful, parameter of smallness in which to expand, viz: $\varepsilon = 0.146\dots$. As defined in Table I, ε provides an estimate of the strength of intercell interactions relative to intracell energies. We calculate the hopping parameters exactly to $O(\varepsilon)$ and the interactions ex-

actly to $O(\varepsilon^2)$. Terms that are higher order in ε are calculable in principle, but they tend to be unreasonably complicated and are not retained in the present work. Already this procedure yields a model that differs in some important aspects from the more familiar one-band t - J and Hubbard-like models.⁴

Far from constituting a special approach, the three-band model of the title⁵ (or some similar version) has to be the starting point for any realistic model of CuO_2 . As commonly formulated,² it is a version of the Hubbard model modified⁶ to incorporate the chemical composition and physical properties of the specific materials. The “symmetric” Coulomb interaction we shall favor here (see below for the definition) is restricted to the copper ions; we shall assume there is no corresponding two-body interaction on the oxygens. Although the form of the Coulomb interaction is not an essential feature of the model, its absence from the oxygen ions is. In fact, the procedure could not be implemented if a two-body force on the oxygen ions were to be included. As this omission is physically justifiable,⁷ the result is not just another “toy” model.

The well-known geometric structure of the copper-oxide planes is easily visualized as follows: coppers lying on a square (sq) lattice of lattice parameter a_0 are separated by the “ligand” (interstitial) oxygen ions. The basic unit cell consists of two oxygen ions and a single copper ion. On the latter, a single $d(x^2 - y^2)$ orbital is involved. For oxygens lying on an horizontal line it is the $p(x)$, and on a vertical, it is the $p(y)$ orbitals which participate—hence the nomenclature “three-band model.”⁵ (Arguably, “three-orbital model” would be more descriptive.) In the simplest version, which is what we use here, an overlap matrix element t_{pd} connects the d orbital to any of its four nearest-neighbor oxygen orbitals or, conversely, an oxygen orbital to either of the two nearest-neighbor copper ion orbitals. Any copper-copper bonds or oxygen-oxygen overlaps are ignored. The two-body Coulomb repulsion U_{dd} is triggered whenever two electrons⁸ or two holes occupy a common copper orbital. The interaction stabilizes the valence of each copper ion at its optimum value Cu^{2+} , the occupancy being set at one electron on the $3d(x^2 - y^2)$ orbital and none on the $4s$ orbital. As there is no such valence stability requirement on the oxygen ions we ignore the Coulomb repulsion of the electrons or holes which occupy them. Thus, with just the two

TABLE I. Intra- and intersite matrix elements $T(R_{ij})$ and their squares, at small distances. This table yields ratios $T(1,1)/T(0,1) \equiv t'/t = -0.17$ and $T(0,2)/T(0,1) \equiv t''/t = -0.10$. Note: $\varepsilon \equiv T(0,1)/T(0) = 0.14622$.

$R(n,m)a_0$	$T(R)$	$T^2(R)$
(0,0)	1.916 182 8	3.6718
($\pm 1,0$) or ($0,\pm 1$)	0.280 185 9	0.0785
($\pm 1,\pm 1$)	-0.047 013 5	0.0022
($\pm 2,0$) or ($0,\pm 2$)	-0.027 450 1	0.0007 ₅

physical quantities t_{pd} and U_{dd} as parameters, the initial three-band Hamiltonian is

$$H = -t_{pd} \sum_{i,\sigma} (c_{i,\sigma}^+ a_{i+\delta,\sigma} + \text{H.c.}) + H_2, \quad (1)$$

where i stands for the position of any of N copper ions on the lattice $(n,m)a_0$, $\delta = (\pm a_0/2, 0)$ or $(0, \pm a_0/2)$, and σ is the electron spin coordinate \uparrow or \downarrow . The ‘‘symmetric’’ two-body interactions are

$$H_2 = U \sum_i [2(c_{i,\uparrow}^+ c_{i,\uparrow} - \frac{1}{2})(c_{i,\downarrow}^+ c_{i,\downarrow} - \frac{1}{2}) + \frac{1}{2}], \quad (2)$$

using $U \equiv \frac{1}{2} U_{dd}$. H_2 involves only Cu sites, as previously noted. Because it is invariant under charge conjugation (i.e., it is ‘‘symmetric’’), the electron occupancy need only be investigated from three to a maximum six electrons/cell. The range 0–3 is related by symmetry.

Actually the physically interesting range is considerably narrower. For p -doped superconductors, e.g., $\text{La}_{2-y}\text{Sr}_y\text{CuO}_4$ (y determining the fraction of electrons removed from the antiferromagnet,⁹) the electron occupancy ranges from 4.5 to 5 electrons per unit cell; for n -doped superconductors, e.g., $\text{Nd}_{2-y}\text{Ce}_y\text{CuO}_4$,⁹ it ranges from 5 to 5.5. At precisely 5 electrons per unit cell the ground state is that of an $S=1/2$ antiferromagnetic insulator of the Néel type;¹⁰ very near 5/cell, it changes into an incommensurate antiferromagnet or a spin glass.¹⁰ At occupancies 4 and 6 the ground states are ordinary nonmagnetic insulating states, which are analyzed completely, to leading orders in ε , in the present paper. However, experimentally, it is at intermediate values between 4.5 and 4.9 and between 5.1–5.5 electrons/cell, that high-temperature superconductivity occurs.

The present work has limited goals. We shall be concerned principally with outlining the nature of the composite charge carriers and calculating the parameters entering their dynamics. We obtain our results by reducing the initial three-band Hamiltonian in a way that is independent of electron concentration. The accuracy is good, but not exact, as we do include interactions as small as $O(\varepsilon^2)$ relative to the largest energies, but no smaller.

Once the form of the model is determined we solve it exactly for $4N$, $4N+1$, and $4N+2$ electrons (or $6N$, $6N-1$, and $6N-2$ electrons.) Although this is rather far from the important region centered about $5N$, the results are interesting. For $4N+2$ electrons the pair ground state, if it were bound, would have s - (and *not* d -) wave symmetry. However, for binding to occur, x would need to be unaccept-

ably large. We extend the two-body solution, using a mean-field BCS (Ref. 11) approximation, to $(4+\nu)N$ electrons. A rather low- T_c superconducting phase, with extended s -wave pairing, is found. Its T_c peaks near $\nu=0.4$. This s -wave phase is superseded by a decidedly more robust d -wave phase in the range $0.5 < \nu < 0.9$.¹² We have determined that this crossover from s -wave to d -wave pairing is rooted in the nearest-neighbor geometry of the superexchange interactions and is unrelated to any other consideration.

It was stated in the recent review of the experimental data on copper-oxide monolayers by Kastner *et al.*¹⁰ that ‘‘...After a decade of research, there is still no consensus as to the correct theory of the kind of superconductivity found in the copper oxides.’’ Perhaps the reason is that while high- T_c superconductivity is found in the range $0.7 < \nu < 1.3$, it is just here that mean-field theory fails, especially in two dimensions. For in this range there is a competition between the metallic/superconducting and antiferromagnetic correlations and fluctuations have proven difficult to analyze. We also note that our calculations, as presented here, are insufficiently refined to explain why the p types are sturdier superconductors than are the n types. These are important issues left, perforce, to future investigations. In the present paper, we concentrate on the p types.

Although a number of extensive computational-numerical studies have brought out the desired correlations, as have some analytical theories (using ‘‘slave’’ bosons or fermions,) these calculations have typically used *ad hoc* values for the model parameters. Therefore they are not directly useful in the present context. Hopefully, future studies will benefit from detailed microscopic relations, such as those we derive in the present work, whereby the ratios of a multitude of effective one-band parameters: $t, t', t'', \dots, V, J, U_{\text{eff}}$ are known as functions of a few variables. In the present simplified case, there is just a single variable x to be determined by fitting to experiment. The composite nature of the charge carriers and the existence of other low-lying composite states, such as the local triplet states, are also all subject to experimental and to numerical verification.

I. AN OVERVIEW OF THE REDUCTION

In our original work¹ we used the lattice Fourier transforms of the vertical [$p(y)$] and horizontal [$p(x)$] orbitals, i.e., the oxygen bands, with which to construct two sets of operators: the α 's and the β 's. Although the α 's hybridize with the coppers (represented by $c_{i,\sigma}$ operators,) the β 's are totally disconnected and constitute a zero-energy, zero-width band capable of accommodating up to two noninteracting electrons per site. Throughout this work, we shall assume the β band is filled. A brief recapitulation of the earlier results together with an extensive discussion of our recent findings follows next.

The Hamiltonian is decomposed into three parts.¹ Aside from $H_\beta=0$ which decouples from the rest and carries no energy, $H_{\text{local}} = \sum_{i=1}^N H_i$ incorporates the hybridization within each cell and $H_{\text{in}} = \frac{1}{2} \sum_i \sum_{j \neq i} H(R_{ij})$ includes all remaining intercell interactions. The individual cells are centered on the N points of the original sq lattice. The lattice parameter remains a_0 .

What renders an accurate reduction possible is the

“smallness” of $H(R_{ij})$ for $R_{ij} \neq 0$, each being explicitly proportional to $T(R_{ij}) = (1/N) \sum_{k \in \text{BZ}} e^{ik \cdot R_{ij}} \omega(k)$, the lattice Fourier transform of the structure factor:

$$\omega(k) = 2\sqrt{\cos^2(1/2)k_x + \cos^2(1/2)k_y}. \quad (3)$$

The T 's are calculated and summarized in Table I. These numbers carry some implications. The cell-diagonal H_i are explicitly $\propto T(0)$ and the magnitudes of their eigenvalues are either $\propto T^2(0)t^*$ or $\propto U$. The intercell H_{ij} are explicitly $\propto T(R_{ij})$, and being off-diagonal in the representation of site-centered states, yield energy corrections $\propto T^2(R_{ij})$. This is smaller than the site-diagonal energies by almost two orders of magnitude. It follows that such multicenter terms as $T(R_{ij})T(R_{jk})T(R_{ki})$ which arise in third or higher-order perturbation theory, are much smaller still and may be safely neglected for our present purposes.

What is more, examination of Table I flags a possible error associated with the neglect of long-distance bonds. Consider the hopping terms listed in the middle column. We invoke an obvious sum rule: $\sum_{\text{all } R} T(R) = 2\sqrt{2}$. However, summing the terms listed in Table I going out as far as third neighbors, we get just 2.739 for this quantity, a discrepancy of ≈ 0.1 . Thus, the total of the contributions from more distant bonds actually exceeds the strength of individual second-nearest-neighbor bonds. This discrepancy strongly suggests a need to retain hopping terms out to long distances.

Not surprisingly, the literature abounds with differing estimates of the magnitudes and the signs for these small bonds. In their numerical study of the spectral density of the charge carriers, Eder, Ohta, and Sawatzky (Ref. 2) used ratios significantly different from those in Table I, viz: $t_{\text{eff}}(1,1)/t_{\text{eff}}(0,1) = t'/t = -0.35$ and $t_{\text{eff}}(0,2)/t_{\text{eff}}(0,1) = t''/t = +0.25$, while in a recent study of the extended van Hove singularity, Yin, Gong, and Leung (Ref. 5) took $t'/t = -0.3$ and $t''/t = 0.2$. It is not known whether inclusion of longer-ranged bonds in either of these calculations would change the sign of the optimum t'' or double the magnitude of the optimum t' .

For the two-body interactions, it is the last column that is relevant. Summing the terms in Table I one obtains 3.995, whereas a sum rule requires $\sum_R T^2(R) = 4$ instead. Clearly the neglect of more distant bonds is easier to justify in this case. Nevertheless, wherever it is practicable we endeavor to retain all the bonds in our calculations.

II. STATES OF A CELL

With two electrons permanently occupying the quiescent β band, one can insert up to an additional four electrons with the aid of the 16 states per cell constructed out of the hybridized α and c operators. These states are listed explicitly below. We distinguish the eight low-energy states ($E \propto -t_{pd}^2/U$) from the eight high-energy states $E \propto U$.

Electron occupancy is measured by a charge quantum number q set arbitrarily to zero at 4 electrons/cell. Generalizing earlier work, we exhibit next all cell-centered eigenstates and eigenvalues exactly, foregoing the simplifications based on $U \gg t_{pd}$. The salient results are recapitulated in Table II for ready reference.

(0) *Two-particle states*: only the two electrons associated

TABLE II. The 16 eigenstates of a cell: a summary. We label each cell state by its leading configuration. In assigning charge we assume the presence, *ab initio*, of two electrons in the zero-width, zero-energy β states, as indicated schematically by $|2\rangle$, on a background of positive ionic charges. The most relevant composite states are indicated by an asterisk (*). These are the low-lying stably bound states, involved in conductivity, superconductivity, and antiferromagnetism, for which we compute the intersite hopping and interaction parameters in the text.

Relative Charge q	State (Schematic)	Degeneracy	E : High $O(U)$, or Low $O(t^*)$
+2	$ 2\rangle$ (0 in text)	1	High
+1	$c_{i,\sigma}^+ 2\rangle$ (1)	2	Low
+1	$\alpha_{i,\sigma}^+ 2\rangle$ (2)	2	High
0	$c_{i,\sigma}^+ \alpha_{i,\sigma'}^+ 2\rangle$ (3 and 5)	4	Low*
0	$c_{i,\uparrow}^+ c_{i,\downarrow}^+ 2\rangle$ (4 and/or 6)	1	High
0	$\alpha_{i,\uparrow}^+ \alpha_{i,\downarrow}^+ 2\rangle$ (4 and/or 6)	1	High
-1	$c_{i,\sigma}^+ \alpha_{i,\uparrow}^+ \alpha_{i,\downarrow}^+ 2\rangle$ (7)	2	Low*
-1	$\alpha_{i,\sigma}^+ c_{i,\uparrow}^+ c_{i,\downarrow}^+ 2\rangle$ (8)	2	High
-2	$c_{i,\uparrow}^+ c_{i,\downarrow}^+ \alpha_{i,\uparrow}^+ \alpha_{i,\downarrow}^+ 2\rangle$ (9)	1	High*

with the β band are present. We define this as $|2,i\rangle$, with i serving to identify the cell, and assign charge quantum number $q = +2$ to this configuration. The energy is high: $E_2 = U$.

(1) *A low-energy three-particle doublet*: $|3\sigma,i\rangle = 1/\sqrt{1+p_3^2}(c_{i,\sigma}^+ + p_3\alpha_{i,\sigma}^+) |2,i\rangle$ with $p_3 = t_{pd}T(0)/(U - E_3)$ and low energy $E_3 = \frac{1}{2}U - \sqrt{(\frac{1}{2}U)^2 + [t_{pd}T(0)]^2} \equiv Ue_3$. This last serves to define the dimensionless energy e_3 . The charge is $q = +1$. The high-energy partner of this state is the following doublet:

(2) $|3\sigma,i\rangle_{\text{exc}} \equiv -1/\sqrt{1+p_3^2}(\alpha_{i,\sigma}^+ - p_3c_{i,\sigma}^+) |2,i\rangle$, high energy, $\tilde{E}_3 = \frac{1}{2}U + \sqrt{(\frac{1}{2}U)^2 + [t_{pd}T(0)]^2} \equiv U\tilde{e}_3$, charge $q = +1$.

(3) There are six four-particle states; all with $q = 0$. The low-energy state is a singlet:

$$|4,i\rangle = \frac{1}{\sqrt{2(1+p_4^2)}} [c_{i,\uparrow}^+ \alpha_{i,\downarrow}^+ + \alpha_{i,\uparrow}^+ c_{i,\downarrow}^+ + p_4(\alpha_{i,\uparrow}^+ \alpha_{i,\downarrow}^+ + c_{i,\uparrow}^+ c_{i,\downarrow}^+)] |2,i\rangle,$$

where $p_4 = 2t_{pd}T(0)/(U - E_4)$ and $E_4 = \frac{1}{2}U - \sqrt{(\frac{1}{2}U)^2 + [2t_{pd}T(0)]^2} \equiv Ue_4$. We use it to form the neutral background in the usual p -type high-temperature superconductors. Its high-energy partner is also a singlet:

(4)

$$|4,i\rangle_{\text{exc}} = -1/\sqrt{2(1+p_4^2)} [\alpha_{i,\uparrow}^+ \alpha_{i,\downarrow}^+ + c_{i,\uparrow}^+ c_{i,\downarrow}^+ - p_4(c_{i,\uparrow}^+ \alpha_{i,\downarrow}^+ + \alpha_{i,\uparrow}^+ c_{i,\downarrow}^+)] |2,i\rangle,$$

with high energy: $\tilde{E}_4 = \frac{1}{2}U + \sqrt{(\frac{1}{2}U)^2 + [2t_{pd}T(0)]^2} \equiv U\tilde{e}_4$.

(5) The $q = 0$ triplets have low energy, $e_{\text{triplet}} = 0$. The first is $|4\uparrow\uparrow,i\rangle = c_{i,\uparrow}^+ \alpha_{i,\uparrow}^+ |2,i\rangle$, the second is $|4\uparrow\downarrow,i\rangle = 1/\sqrt{2}(c_{i,\uparrow}^+ \alpha_{i,\downarrow}^+ + c_{i,\downarrow}^+ \alpha_{i,\uparrow}^+) |2,i\rangle$, and the third is $|4\downarrow\downarrow,i\rangle = c_{i,\downarrow}^+ \alpha_{i,\downarrow}^+ |2,i\rangle$.

(6) The final member of the $q=0$ family is a singlet of high energy: $|4',i\rangle_{\text{exc}} = 1/\sqrt{2}(c_{i,\uparrow}^+c_{i,\downarrow}^+ - \alpha_{i,\uparrow}^+\alpha_{i,\downarrow}^+)|2,i\rangle$, with energy $E_4' = U$, $e_4' = 1$.

(7) Two sets of doublets belong to $q=-1$. The low-energy doublet is the more important: $|5\sigma,i\rangle \equiv 1/\sqrt{1+p_5^2}(c_{i,\sigma}^+\alpha_{i,-\sigma}^+ + p_5c_{i,\sigma}^+c_{i,-\sigma}^+\alpha_{i,\sigma}^+)|2,i\rangle$, with $p_5 = p_3$ and $e_5 = e_3$. This is the ‘‘composite’’ state most directly involved in charge transport, antiferromagnetism, and superconductivity in CuO_2 .

(8) Its high-energy partner is $|5\sigma,i\rangle_{\text{exc}} \equiv -1/\sqrt{1+p_5^2}(c_{i,\sigma}^+c_{i,-\sigma}^+\alpha_{i,\sigma}^+ - p_5c_{i,\sigma}^+\alpha_{i,-\sigma}^+\alpha_{i,\sigma}^+)|2,i\rangle$, $\bar{e}_5 = \bar{e}_3$.

(9) Finally, the state of maximal occupancy is the singlet state: $|6,i\rangle = c_{i,\uparrow}^+c_{i,\downarrow}^+\alpha_{i,\uparrow}^+\alpha_{i,\downarrow}^+|2,i\rangle$. It has high energy, $E_6 = U$, and a charge number $q = -2$.

For any specified q and spin the stable configuration of any cell is the one having the lowest energy compatible with these quantum numbers. Being subject to decay, higher-energy states are intrinsically unstable.¹³ In equilibrium only the stable states are observed. This ‘‘stability principle’’ can be used to determine the equilibrium configurations as electrons are added to, or subtracted from, the material. The following example illustrates the principle for fewer than five electrons per cell, i.e., in the p -type materials.

For this case the most useful starting point or ‘‘vacuum’’ is a product state of Zhang-Rice singlets¹⁴ [the low-energy $|4,i\rangle$'s], one at each site. This configuration has total charge $Q = \sum_i q_i = 0$, by definition. Adding an electron to the i th site costs a minimum energy $E_5 - E_4$ and transforms it to a doublet $|5\sigma,i\rangle$, (7 above,) with $q_i = -1$ and $\sigma = \uparrow$ or \downarrow . Amusingly, removal of an electron from this vacuum proceeds by an entirely different process.¹⁵

The addition of a larger number νN of electrons decreases the total charge Q from its initial value of zero to $-\nu N$ and introduces doublets of type 7, the ‘‘composite particles’’ of our theory, on νN distinct sites. There is no ambiguity in this assignment as excited doublets of type 8 are never advantageous and singlet states of type 9 are always more costly in energy. In fact, $2E_5 \ll U + E_4$ regardless of the value of x . In the p -type materials the states 9 are only accessed virtually. However, they do play an important role once $\nu > 1$, in the n -type materials.

At $\nu = 1$ precisely, the ground state is that of a spin-1/2 antiferromagnetic insulator with a superexchange parameter $J(R_{ij})$, connecting spins at distinct sites R_i and R_j .¹⁰ It is a ‘‘charge-transfer’’-type insulator not because of a filled band, but because charge transport, which we calculate next, is prohibited between any two cells which have the same valence.

III. INCLUDING H_{ij} , CHOOSING ENERGY UNITS

Both transport and intersite interactions are mediated by H_{ij} , explicitly proportional to the ‘‘bare’’ hopping parameters $-t_{pd}T(R_{ij})$:

$$H_{ij} = -t_{pd}T(R_{ij}) \sum_{\sigma} \{(c_{i,\sigma}^+\alpha_{j,\sigma} + \text{H.c.}) + (c_{j,\sigma}^+\alpha_{i,\sigma} + \text{H.c.})\}. \quad (4)$$

Now, H_{ij} has matrix elements connecting any initial configuration of a product state such as $|m,i\rangle \otimes |m',j\rangle$, to as many as 255 target configurations. Most of these vanish, as two conservation laws serve to greatly reduce the number of allowed target configurations; to wit: H_{ij} in Eq. (4) conserves both $\Omega_{ij} = \sum_{\sigma} (c_{i,\sigma}^+c_{i,\sigma} + \alpha_{j,\sigma}^+\alpha_{j,\sigma})$ and Ω_{ji} separately, hence it conserves total charge $Q_{ij} = \Omega_{ij} + \Omega_{ji}$ and ‘‘pseudo-charge’’ $Q'_{ij} = \Omega_{ij} - \Omega_{ji}$ for the two sites. Moreover, H_{ij} conserves the joint (total) spin angular momentum of the two sites.

As an example of the use of these selection rules, consider the effects of $H_{\text{int}} = \frac{1}{2} \sum H_{ij}$ on the energy of the ‘‘vacuum’’ state, in second-order perturbation theory. The selection rules permit each initial state $|0\rangle \equiv |4,i\rangle \otimes |4,j\rangle$ to connect to just four target states, thereby eliminating several hundred possibilities. The four finalist candidate states are

$$|1\rangle \equiv \frac{1}{\sqrt{2}} \{|3\uparrow,i\rangle \otimes |5\downarrow,j\rangle - |3\downarrow,i\rangle \otimes |5\uparrow,j\rangle\},$$

$$|2\rangle \equiv \frac{1}{\sqrt{2}} \{|3\uparrow,i\rangle_{\text{exc}} \otimes |5\downarrow,j\rangle - |3\downarrow,i\rangle_{\text{exc}} \otimes |5\uparrow,j\rangle\},$$

$$|3\rangle \equiv \frac{1}{\sqrt{2}} \{|3\uparrow,i\rangle \otimes |5\downarrow,j\rangle_{\text{exc}} - |3\downarrow,i\rangle \otimes |5\uparrow,j\rangle_{\text{exc}}\},$$

$$|4\rangle \equiv \frac{1}{\sqrt{2}} \{|3\uparrow,i\rangle_{\text{exc}} \otimes |5\downarrow,j\rangle_{\text{exc}} - |3\downarrow,i\rangle_{\text{exc}} \otimes |5\uparrow,j\rangle_{\text{exc}}\}.$$

Of these, the matrix elements $(\langle 1|H_{ij}|0\rangle) = (\langle 4|H_{ij}|0\rangle) = 0$ both vanish by symmetry. Hence, the entire second-order contribution to the energy of $|0\rangle$ comes from just two matrix elements, those connecting $|0\rangle$ with $|2\rangle$ and with $|3\rangle$. We then calculate,

$$\Delta E_{44}(R_{ij}) = -\frac{2t_{pd}^2 T^2(R_{ij})}{U - 2E_4} \left(\frac{1 - p_4^2}{1 + p_4^2} \right)^2.$$

Now, in expressing quantities such as this, it is natural to use $t^* \equiv t_{pd}^2/2U$ as the unit of energy (just as it was in the limit model), and to define $x \equiv t_{pd}T(0)/U$ as the sole, non-trivial, parameter of the theory. Assuming only $|t_{pd}| < U_{dd}$ we see the widest physically permissible range for this parameter is $0 < x < 3.8$. In this work we assume x is $O(1)$, i.e., neither $\rightarrow 0$ nor $\rightarrow \infty$.

With these substitutions ΔE simplifies to

$$\Delta E_{44}(R_{ij}) = -\frac{4t^*T^2(R_{ij})}{1 - 2e_4} \left(\frac{1 - p_4^2}{1 + p_4^2} \right)^2 = -\frac{4t^*T^2(R_{ij})}{(1 + 16x^2)^{3/2}}, \quad (5)$$

so that the total energy of the plane of 4's is

$$E_0 = NE_4 + \frac{1}{2}N \sum_{R \neq 0} \Delta E_{44}(R) \\ = Nt^* \left\{ \frac{T^2(0)}{x^2} [1 - \sqrt{1 + 16x^2}] - \frac{2K_0^2}{(1 + 16x^2)^{3/2}} \right\}, \quad (6)$$

where $K_0^2 \equiv \sum_{R \neq 0} T^2(R) = 4 - T^2(0) = 0.3282\dots$ sums all ΔE_{44} interactions.

IV. AN ERROR ANALYSIS

The above allows us to estimate some errors intrinsic to this theory. At $x=0$, the ratio of the total two-site contributions ΔE_{44} to that of the site-diagonal energy is $0.3282/(4 \times 3.6718) = 2.2\%$; at $x=1$ it has dropped to $<1\%$. Third- and higher-order contributions involving two, three or more sites, each carry additional factors of $T(R)$ with $R \neq 0$. Regardless of the value of x , all are smaller than the ΔE_{44} contributions by additional factors of ε .

The original limit model¹ was anchored to the limit $x \rightarrow 0$. We have now determined that x need not be zero, nor even small. The true parameter of smallness, as mentioned in the Introduction, is ε . To leading order in ε the energies consist of just the site-diagonal terms, which are computed exactly, and of the more numerous two-site interactions, which are computed to $O(\varepsilon^2)$. In addition, off-diagonal terms connect degenerate configurations. These off-diagonal terms are responsible both for charge transport and for the ‘‘transverse’’ interactions in superexchange, i.e., $\frac{1}{2}J(R_{ij})(S_i^+ S_j^- + \text{H.c.})$. We examine the transport parameters first and the exchange terms subsequently.

V. CHARGE TRANSPORT

Charge transport necessitates charge transfer. Consider the product state of two sites having q 's which differ by ± 1 , e.g., $|0\rangle \equiv |4, i\rangle \otimes |5 \uparrow, j\rangle$. This particular initial state connects to 11 target states consistent with the selection rules, of which just one, the permutation: $|1\rangle \equiv |5 \uparrow, i\rangle \otimes |4, j\rangle$, is degenerate with $|0\rangle$. For the given initial state, this is the only target state involved in real (not virtual) charge transfer from site R_j to site R_i , to leading order in ε .

The matrix element of H_{ij} connecting $|0\rangle$ to $|1\rangle$ yields the ‘‘effective hopping’’ parameter, which allows a five-electron cell with $q = -1$ to propagate in the background of cells having $q = 0$.¹⁶ After some calculation we find this effective hopping parameter to carry a sign which is explicitly opposite to that of the ‘‘bare’’ matrix element in Eq. (4):

$$t_{\text{eff}}^{54}(R_{ij}) = +2t^*T(0)T(R_{ij}) \frac{(p_4 + p_5)(1 + p_4 p_5)}{x(1 + p_4^2)(1 + p_5^2)} \equiv t^* \Phi_{54}(x)T(R_{ij}). \quad (7)$$

This expression also serves to define $\Phi_{54}(x)$, used in later expressions. By symmetry, the hopping parameter for so-called ‘‘holes,’’ i.e., for the propagation of a $q = 0$ cell of type $|4, i\rangle$ in an antiferromagnetic sea of $q = -1$ cells of type $|5 \sigma, j\rangle$, is numerically the same as above, being $\Phi_{45}(x) = \Phi_{54}(x)$. This remark is germane for those theories or numerical studies that examine the propagation and interactions of such ‘‘holes’’ in the highly correlated region near the antiferromagnetic point.¹⁷

The propagation of a $|5 \sigma, i\rangle$ in a sea of $|6, j\rangle$'s (or vice versa) is required for the study of n -doped materials. In this case the sign agrees with that of the bare quantity in Eq. (4),

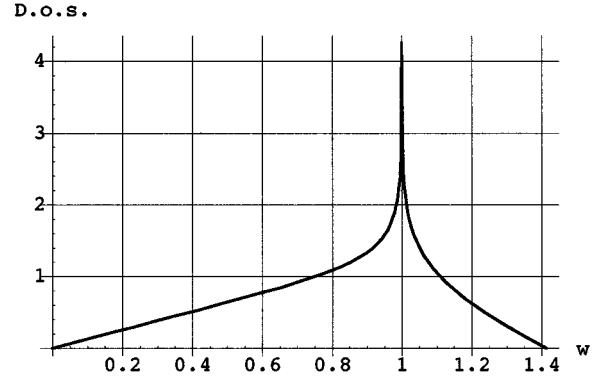


FIG. 1. Dimensionless one-particle density of states $\rho(w)$ appropriate to $\omega(k)$ in Eq. (3).

$$t_{\text{eff}}^{56}(R_{ij}) = -4t^*T(0)T(R_{ij}) \frac{p_5}{x(1 + p_5^2)} \equiv t^* \Phi_{56}(x)T(R_{ij}). \quad (8)$$

The difference in signs between the two scenarios is significant. Insofar as it permutes the density of states at the respective band edges it distinguishes the hopping behavior of a dilute gas of 5's in a background of 4's from that in a background of 6's. However, because $T(R_{ij})$ converges so slowly, we should not consider just nearest- and next-nearest-neighbor matrix elements. Rather, we shall construct an ‘‘effective band structure’’ which retains them all. In this respect our reduction differs from the t - t' - J models of the literature⁴ in which only nearest- and next-nearest-neighbor hops are retained. What is more, the ratio of the various t 's is not arbitrary but is a consequence of the hybridization, as in Table I.

The above transfer-matrix elements are first order in the $T(R_{ij})$, hence in ε . Clearly there are three-center terms such as $\sum_k T(R_{ik})T(R_{kj})$ which are $\propto \varepsilon^2$ and four-center terms which are higher-order still. These can interfere with the first-order hopping terms. Preliminary results show that three-center terms can significantly modify Eqs. (7), (8), and (10), hence Figs. 1 and 2. The modifications depend on the value of ν . We shall report on this elsewhere.

VI. WEAK-COUPPLING LIMIT

It is instructive to solve the three-band model of noninteracting electrons, i.e., to examine the weak-coupling limit. One sets $H_2 = 0$ at the outset and solves for the free fermion states of H . (The algebraic details are left as an exercise for the reader.)

Three bands are found. One is the β band, consisting of the decoupled linear combination of oxygen orbitals. The other two have dispersion $\varepsilon_{\pm}(k) = \pm |t_{pd}| \omega(k)$. For an electron filling factor in the range $\nu = 4 - 6$ electrons/cell, both the β band and the $-|t_{pd}| \omega(k)$ band are filled. Only the $+|t_{pd}| \omega(k)$ band is partly occupied. Except for trivial scale factors, the density of states of this last is that of Fig. 1. In the range $\nu = 5 - 6$ electrons per cell it is desirable to describe transport in terms of holes. There the density of states is inverted (i.e., the sign of the Bloch energies is changed).

As we shall see shortly, in strong coupling the analysis is practically identical. The principal differences, as seen im-

mediately below, consist of the replacement of $\varepsilon_+(k)$ above by $t^*\Phi_{54}\omega(k)$ in the range $\nu=4-5$, and by $t^*\Phi_{56}\omega(k)$ (which carries the change in sign intrinsically) in the range 5–6. In addition, in strong coupling the entities are subject to interactions, as calculated below, which could modify their dispersion considerably.

VII. SELF-ENERGIES AND BLOCH ENERGIES

The total energy E_0 calculated in Eq. (6) is an absolute minimum.¹⁸ The replacement of a single $|4,i\rangle$ cell by a $|5\uparrow j\rangle$ raises it in the amount:

$$\Delta E_5 = E_5 - E_4 + \sum_R [\Delta E_{54}(R) - \Delta E_{44}(R)].$$

We call this the self-energy of the composite particle, i.e., of the stable charged cell ($q = -1$). The summand $\Delta E_{44}(R)$ was given in Eq. (5), while $\Delta E_{54}(R)$ is the energy of interaction between the $q = -1$ cell $|5\sigma, j\rangle$ and a $q = 0$ cell $|4, i\rangle$ at distance R . After some algebra, we find the latter to be

$$\begin{aligned} \Delta E_{54}(R) = & -\frac{1}{2}T^2(R)t^* \left\{ \frac{1}{1-2e_4} \left(\frac{1-p_4^2}{1+p_4^2} \right)^2 \right. \\ & + \frac{1}{1-2e_5} \left(\frac{1-p_5^2}{1+p_5^2} \right)^2 + \frac{3}{1-e_4} \left(\frac{1}{1+p_4^2} \right) \left(\frac{1-p_5^2}{1+p_5^2} \right)^2 \\ & + \frac{3}{-e_4} \left(\frac{p_4^2}{1+p_4^2} \right) \left(\frac{1-p_5^2}{1+p_5^2} \right)^2 \\ & + \frac{3}{2-e_4-2e_5} \left(\frac{(2p_5-p_4-p_4p_5^2)^2}{(1+p_4^2)(1+p_5^2)^2} \right) \\ & \left. + \frac{3}{1-e_4-2e_5} \left(\frac{(1+p_5^2-2p_4p_5)^2}{(1+p_4^2)(1+p_5^2)^2} \right) \right\}. \quad (9) \end{aligned}$$

We subtract $\Delta E_{44}(R)$ and sum on R . It is noteworthy that the resulting sum lowers the bare cell energy $E_5 - E_4$ by only 2.5% at most. Higher-order corrections carry additional factors $O(\varepsilon)$ and are justifiably neglected.

In first-order perturbation theory the ‘‘effective’’ band structure of the composite particle is found using the appropriate plane-wave linear combination of degenerate states. This leads to the Fourier transform of $T(R)$, i.e., $\omega(k)$. Then the Bloch energy $\Delta E_5(k)$ is

$$\Delta E_5(k) = \Delta E_5 + t^*\Phi_{54}(x)[\omega(k) - T(0)], \quad (10)$$

obtained by combining Eq. (7) and $\omega(k)$ given in Eq. (3). This expression incorporates the self-energy ΔE_5 . Note that $T(0) = \langle \omega(k) \rangle_{\text{BZ}}$ is the average or ‘‘center of gravity’’ of $\omega(k)$ over the Brillouin zone.

The dimensionless density of states

$$\rho(w) \equiv \frac{1}{N} \sum_k \delta(w - \frac{1}{2}\omega(k))$$

corresponding to this dispersion is plotted in Fig. 1. We draw the reader’s attention to several interesting features: (A) the van Hove logarithmic ‘‘nesting’’ singularity, at $w = 1$, lies higher than the half-filling point located at $w_{1/2} \approx 0.874$. (B)

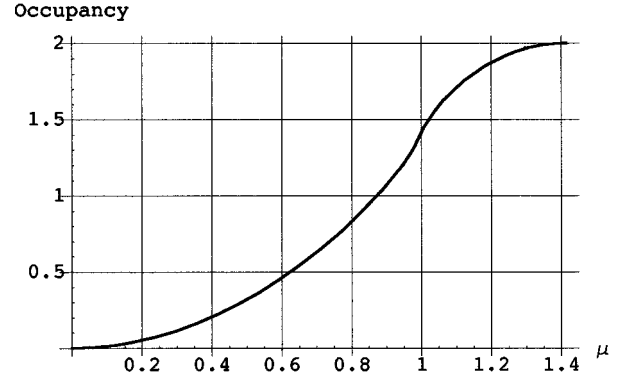


FIG. 2. Occupancy ν as a function of dimensionless Fermi energy μ , based on the density of states in Fig. 1. (The average number of particles *per* cell is $4 + \nu$.)

At 85% of half-filling, $w = 0.810$. (C) The center of gravity of the band is at 0.908, and (D) its maximum is at $\sqrt{2} = 2.828$.

We show occupancy (ν) as a function of a dimensionless Fermi level (μ) in Fig. 2. Figures 1 and 2 are relevant to the one-body properties of the composite charge carriers and also characterize the electronic band structure in weak coupling, as discussed in the preceding section.

At high density [$\nu = O(1)$] the composite particles will interact strongly with one another, prior to their condensation into the correlated insulating antiferromagnetic phase. The features labeled (A)–(D) above, which are exact in weak coupling, can be affected by such interactions. Even the position of the van Hove singularity relative to $w_{1/2}$ may be reversed for the quasiparticles in strong coupling, if the two-body correlations^{5,19} are properly taken into account.

The bandwidth $W_{\text{eff}} = \Delta E_5(\pi, \pi) - \Delta E_5(0, 0)$ is a monotonically decreasing function of x . Its maximum is $\approx 32.5t^*$ at $x = 0$. Using Eq. (10) we plot $w_{\text{eff}}(x) = W_{\text{eff}}/t^*$ as a function of x in Fig. 3.

Figure 1 illustrates a substantial asymmetry between bottom and top of the band. This asymmetry can also be examined analytically. Consider a dilute ‘‘gas’’ of 5’s in a background of 4’s. Expand Eq. (10) near the band minimum at $k_\pi = (\pi, \pi)$. Measuring k from k_π , we obtain

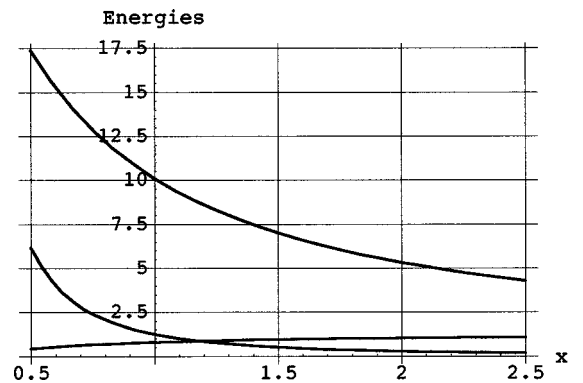


FIG. 3. Energies (in units of t^*) as functions of the parameter x . Top curve: bandwidth $w_{\text{eff}}(x)$. Descending middle curve: zero-range repulsion $u(x)$. Ascending curve: $J(0,1) - V(0,1) = T^2(0,1)[\mathbf{J}(x) - \mathbf{V}(x)] \approx T^2(0,1)\mathbf{J}(x)$, measuring the *net* attractive potential of two nearest-neighbor composite particles in a spin singlet state.

$$\Delta E_5(k) = \Delta E_5(k_\pi) + C|k|. \quad (11)$$

In two dimensions, linear dispersion implies a linear density-of-states: $\rho(w) \propto w$. Surely this unusual dispersion relates to some or all of the anomalous properties of the material. In fact, a low density of states interferes with Cooper pairing at low carrier densities and, in conjunction with a zero-range potential we discuss below, inhibits the formation of bound states in a dilute gas of 5's.²⁰ Next, we examine the two-cell interactions, which come in two varieties: scalar and vector (exchange).

VIII. SCALAR TWO-BODY POTENTIALS

If two 5 \uparrow 's are introduced into the sea of 4's, the one at R_i and the other at R_j ,²¹ the total excitation energy $\Delta E_{\uparrow\uparrow}$ depends on their separation and is not precisely equal to the constant $2\Delta E_5$. The difference defines the two-body scalar effective potential energy, a nontrivial function of x :

$$V_{55,4}(R_{ij}) = \Delta E_{\uparrow\uparrow}(R_{ij}) + \Delta E_{44}(R_{ij}) - 2\Delta E_{54}(R_{ij}). \quad (12)$$

For the interesting and nontrivial case of p -type materials, this constitutes a weak repulsive potential.²² In the nontrivial case, we find

$$\begin{aligned} V_{55,4}(R_{ij}) = & 3t^*T^2(R_{ij}) \left\{ -\frac{1}{1-2e_4} \left(\frac{(1-p_4^2)}{(1+p_4^2)} \right)^2 \right. \\ & - \frac{1}{1-2e_5} \left(\frac{(1-p_5^2)}{(1+p_5^2)} \right)^2 + \frac{1}{(1+p_4^2)(1+p_5^2)^2} \\ & \times \left[\frac{(1-p_5^2)^2}{1-e_4} + \frac{(2p_5-p_4-p_4p_5^2)^2}{2-e_4-2e_5} \right. \\ & \left. \left. + \frac{(1+p_5^2-2p_4p_5)^2}{1-e_4-2e_5} + \frac{p_4^2(1-p_5^2)^2}{-e_4} \right] \right\} \\ \equiv & t^*T^2(R_{ij})\mathbf{V}(x). \end{aligned} \quad (12a)$$

$\mathbf{V}(x)$ decreases fairly rapidly from its maximum value 3 at $x=0$,²³ to insignificantly small values at all $x \geq 1$. Because $T^2(R)$ is small and decreases rapidly with distance, $V_{55}(R_{ij})$ is totally insignificant beyond nearest-neighbor sites. In any event, for $x \geq 0.21$ this scalar potential is exceeded by the attractive force of superexchange computed in the following section. The magnitude of the attractive potential for a single pair, $J(0,1) - V(0,1)$, is plotted in Fig. 3. The x dependences of $\mathbf{V}(x)$ and $\mathbf{J}(x)$ are illustrated in Figs. 4 and 5, respectively.

IX. EXCHANGE FORCES

The interaction energy of two 5's of specifically opposite spins is $V_{\uparrow\downarrow}(R_{ij}) = \Delta E_{\uparrow\downarrow}(R_{ij}) + \Delta E_{44}(R_{ij}) - 2\Delta E_{54}(R_{ij})$. We shall identify this as a Heisenberg interaction. After computing $\Delta E_{\uparrow\downarrow}(R_{ij})$, which has contributions from target states $|4,i\rangle \otimes |6,j\rangle$ and $|4,i\rangle_{\text{exc}} \otimes |6,j\rangle$ (and similar configurations with $i \leftrightarrow j$), we finally derive the superexchange parameter $J(R_{ij}) \equiv 2[V_{55,4}(R_{ij}) - V_{\uparrow\downarrow}(R_{ij})]$, which is the coefficient in $J(R_{ij})(S_i \cdot S_j - \frac{1}{4})$. It is

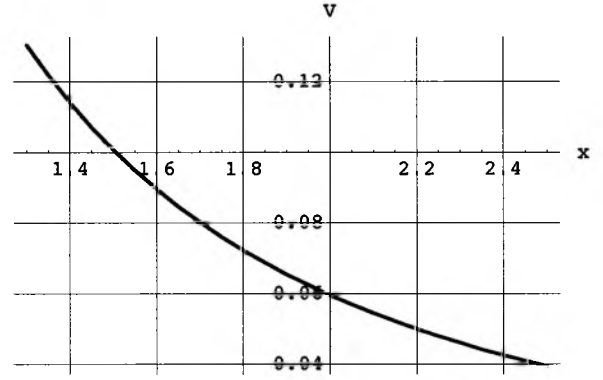


FIG. 4. Detail of Fig. 3: $V(0,1)/t^* = T^2(0,1)\mathbf{V}(x)$.

$$\begin{aligned} J(R_{ij}) = & 4t^*T^2(R_{ij}) \left\{ -\frac{1}{1-2e_5} \left(\frac{(1-p_5^2)}{(1+p_5^2)} \right)^2 \right. \\ & + \frac{1}{(1+p_4^2)(1+p_5^2)^2} \left[\frac{(2p_5-p_4-p_4p_5^2)^2}{2-e_4-2e_5} \right. \\ & \left. \left. + \frac{(1+p_5^2+2p_4p_5)^2}{1+e_4-2e_5} \right] \right\} \equiv t^*T^2(R_{ij})\mathbf{J}(x). \end{aligned} \quad (13)$$

Alternatively, the superexchange parameter J can be found by subtracting the energy of a singlet pair from that of the triplet calculated in the previous section, with an identical result.

The superexchange interaction $J(R_{ij})$ pertains to the pair of sites i and j in question and is independent of the state of all the other sites. Hence it is the same whether the two 5's are imbedded in a sea of 4's or 6's, and one needs not distinguish the two scenarios. Like the scalar potential $V(R_{ij})$, it is also principally confined to nearest-neighbor cells by a factor $T^2(R_{ij})$ which decreases rapidly with distance. Because $\mathbf{J}(0)=0$, superexchange was performed absent in the original version of the limit model.

In principle we could also obtain coefficients of three-body spin terms $S_i \cdot (S_j \times S_k)$, but as three-center interactions are explicitly higher order in ε they are well beyond the scope of this theory and are omitted. Experimentally too, the spin-wave dispersion in the antiferromagnetic insulator ($\nu=1$) has been extremely well fitted with just nearest-neighbor interactions.¹⁰

Unlike an attractive scalar interaction, the two-spin superexchange interaction cannot promote a substantial charge

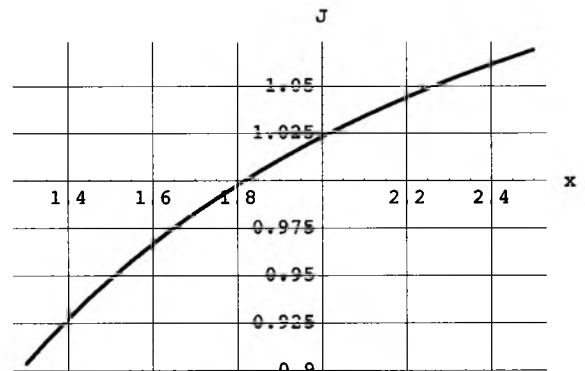


FIG. 5. Detail of Fig. 3: $J(0,1)/t^* = T^2(0,1)\mathbf{J}(x)$.

density or dielectric instability. However, it can render the sea of composite fermions unstable against antiferromagnetism, whether commensurate or incommensurate or, render the metallic phase unstable against superconductivity. Its magnitude (≈ 0.1 eV) in the copper-oxide materials has been extensively documented.¹⁰

For two 5's in a mutual spin singlet configuration at distance R in a p -type material, $V(R) - J(R)$ is the interaction potential. Our calculations show this interaction to be attractive for all $x > 0.21$. Figure 3 compares the magnitude $|V(R) - J(R)|$, evaluated at nearest-neighbor distance, with other quantities.

X. ADDITIVITY OF POTENTIALS: AN EFFECTIVE HAMILTONIAN

Within the present scheme all two-body potentials and the kinetic (i.e., hopping) energies are additive. Nonadditive three- and four-body forces and corrections to hopping matrix elements are all higher order in ε than those which are retained. It is now possible to restrict attention to the 5's, which are the composite charge carriers of the model, and to analyze their motions and interactions in a background of all 4's or all 6's, by means of a generic Hamiltonian valid in either n - or p -type materials:

$$H_{\text{eff}} = t^* \left\{ \Phi(x) \sum_{i,j,\sigma} T(R_{ij}) (d_{i,\sigma}^+ d_{j,\sigma} + \text{H.c.}) \right. \\ \left. + \frac{1}{2} \mathbf{V}(x) \sum_{i,j} T^2(R_{ij}) n_i n_j + \mathbf{u}(x) \sum_i n_{i,\uparrow} n_{i,\downarrow} \right. \\ \left. + \frac{1}{2} \mathbf{J}(x) \sum_{i,j} T^2(R_{ij}) (S_i \cdot S_j - \frac{1}{4} n_i n_j) \right\}, \quad (14)$$

in which d^+ replaces a background cell by a 5. The background cells are the 4's for p -type doping, the 6's for the n -type. Conversely, d annihilates a 5 and replaces it by the appropriate background cell. The quantities Φ differ for n - and p -type materials, as do \mathbf{V} and \mathbf{u} . Only \mathbf{J} remains the same in both cases.

Being associated with an odd number of fermions, the d 's satisfy anticommutation relations. They live on the sq lattice. The occupation number operators are $n_{i,\sigma} = d_{i,\sigma}^+ d_{i,\sigma}$ and $n_i = \sum_{\sigma} n_{i,\sigma}$. Spin operators S_i act on the spin degrees of freedom of the 5's. They are constructed with the aid of the Pauli matrices σ as follows: $S_i = \frac{1}{2} (d^+ \cdot \sigma \cdot d)$, where $(d^+) \equiv (d_{i,\uparrow}^+, d_{i,\downarrow}^+)$ and $(d) \equiv (d_{i,\uparrow}, d_{i,\downarrow})$. The resemblance of Eq. (14) to the t - J model is somewhat coincidental, as the hopping range is effectively unbounded and the zero-range potential $U_{\text{eff}}(x) = t^* \mathbf{u}(x)$ might not necessarily qualify as a hard core.

However, this reduction does not tell the whole story. Any of the one-cell excitations listed in Table II may contribute to thermal, transport, and optical properties. There are many mentions of "excitons" in the literature, which just relate to these excited states. However, if we wish to understand conductivity, superconductivity, and antiferromagnetism the reduced one-band model H_{eff} provides the most pertinent information.

All energies now scale explicitly with t^* and all, except for the zero-range potential $U_{\text{eff}}(x)$, have now been derived

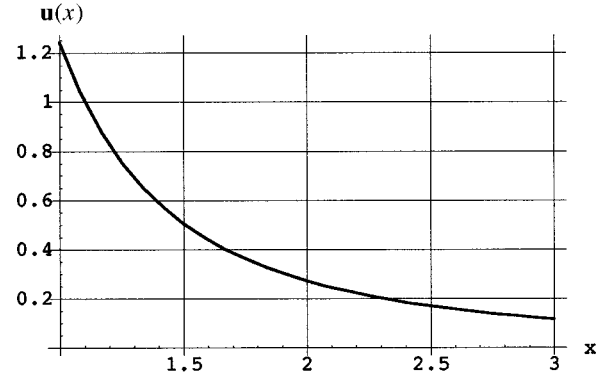


FIG. 6. Detail of Fig. 3: $\mathbf{u}(x)$.

explicitly, as functions of x and R . Finally, we turn to this zero-range interaction potential, the "effective Hubbard interaction," in the following section.

XI. HARD CORE OR SOFT?

Figure 3 compares the zero-range interaction $\mathbf{u}(x)$ (see middle curve) with the other relevant energies in p -type materials as function of x . This quantity is also shown in greater detail in Fig. 6. (A similar calculation of \mathbf{u} in the n -type materials is omitted here for the sake of brevity.) We find that although it is indeed a "hard core" potential at small x , $\mathbf{u}(x)$ rapidly becomes insignificant for $x > 1.5$. In that case, this "soft core" can be handled in perturbation theory, except for filling factor ν near 1.

The explanation of why some antiferromagnetic lattices "melt" at doping levels as small as a few %, may be connected to this observation. (For example, $\text{La}_2\text{CuO}_{4+\delta}$ an antiferromagnetic insulator with Néel temperature 300 K at $\delta=0$, becomes metallic at $\delta=0.02$.)²⁴ If it is sufficiently small, $\mathbf{u}(x)$ fails to stabilize the antiferromagnetic insulator and favors the metallic phase, once ν deviates from 1. We next derive $\mathbf{u}(x)$ in two stages.

First we calculate the contribution $\Delta E_{55}(R_{ij})$ to the interaction energy of a singlet pair of 5's, $|ij\rangle \equiv \sqrt{1/2} \{ |5\uparrow, i\rangle \otimes |5\downarrow, j\rangle - |5\downarrow, i\rangle \otimes |5\uparrow, j\rangle \}$, arising from admixing with the two target states $\sqrt{1/2} \{ |6, i\rangle \otimes |4, j\rangle + |4, i\rangle \otimes |6, j\rangle \}$ or $\sqrt{1/2} \{ |6, i\rangle \otimes |4, j\rangle_{\text{exc}} + |4, i\rangle_{\text{exc}} \otimes |6, j\rangle \}$, both of which correspond to $q_i = -2$ and $q_j = 0$ (or vice versa). By direct calculation, to second order in ε we find

$$\Delta E_{55}(R_{ij}) = -T^2(R_{ij}) \left\{ \frac{M_1^2}{U + E_4 - 2E_5} + \frac{M_2^2}{2U - E_4 - 2E_5} \right\}, \quad (15)$$

where

$$M_1 = - \frac{2t(1 + 2p_4 p_5 + p_5^2)}{(1 + p_5^2) \sqrt{2(1 + p_4^2)}}, \\ M_2 = - \frac{2t(p_4 - 2p_5 + p_4 p_5^2)}{(1 + p_5^2) \sqrt{2(1 + p_4^2)}}.$$

We now define U_{eff} by comparison with the one-band Hubbard model used in semiphenomenological studies in high- T_c superconductivity since the early days of the field.²⁵ Assum-

ing the matrix element for the process $5+5 \rightarrow 4+6$ is exactly equal to the one-particle hopping $t_{\text{eff}} = t^* \Phi(x) T(R_{ij})$ and the excitation energy is a unique U_{eff} , the interaction energy in this Hubbard model would be

$$\Delta E_{55}(R_{ij}) = -2 \frac{t_{\text{eff}}^2}{U_{\text{eff}}},$$

with

$$t_{\text{eff}} = t^* \Phi(x) T(R_{ij}). \quad (16)$$

Finally, equating Eq. (15) to Eq. (16) yields the desired quantity, $U_{\text{eff}} \equiv t^* \mathbf{u}(x)$.

XII. MANY-BODY EIGENSTATES

Now that all the parameters entering Eq. (14) have been determined, we face the question of how to construct the eigenstates and eigenvalues of H_{eff} . Although an exact solution is perfectly feasible for two composite particles (5's) in a sea of 4's or 6's, it is essentially impossible to find a closed-form solution for more than 2. Therefore, at finite density we shall appeal to a mean-field BCS approximation for our preliminary results.

Recall that a pair of 5's in a relative spin triplet configuration is subject only to weak but repulsive potentials. Thus, if there is a bound state it must be sought in the singlet sector.

Because of the rapid dropoff of $T^2(R_{ij})$ with increasing distance R_{ij} , it is sensible to restrict the potentials just to the on-site and nearest-neighbor interactions appropriate to a pair of fermions in a spin singlet state.

However, the *hopping* matrix elements, being proportional to $T(R_{ij})$, do not drop off as rapidly as do their squares. In fact, it is necessary to retain all non-nearest-neighbor hopping terms. Fortunately, it is possible to reformulate the problem in momentum space with the aid of Eq. (10).

A low-lying two-body bound state may develop once x exceeds a critical value. This critical value is dependent on the relative strengths of J , U_{eff} and of the hopping matrix elements, all of which depend on x . The bound state is written in the form $(1/\sqrt{N}) \sum_k \Psi_k d_{\uparrow}^+(k) d_{\downarrow}^+(k) |0\rangle$, where $|0\rangle$ stands for the "vacuum" (product state of all 4's,) k is measured from the band minimum at (π, π) for p -type materials, and Ψ_k is an even function of k satisfying the integral equation

$$\begin{aligned} & [2\varepsilon(k) - E] \Psi_k + [\mathbf{V}(x) - \mathbf{J}(x)] T^2(1,0) \frac{1}{N} \\ & \times \sum_{k'} [\cos(k_x - k'_x) + \cos(k_y - k'_y)] \Psi_{k'} \\ & + u_{\text{eff}}(x) \frac{1}{N} \sum_{k'} \Psi_{k'} = 0, \end{aligned} \quad (17)$$

where for the p -type materials $\varepsilon(k) \equiv \Delta E_5(k_x - \pi, k_y - \pi) - \Delta E_5(\pi, \pi)$ and the binding energy is $-E \geq 0$. Noting that the kernel is the sum of two separable kernels, one infers the form of the wave function:

$$\Psi_k = \text{norm} \times \frac{a + b \cos k_x + c \cos k_y}{2\varepsilon(k) + |E|}. \quad (18)$$

Here $b = c$ defines the "extended s -wave" solution, and $a = 0, b = -c$, the d -wave solution. (The odd p -wave solutions correspond to spin triplets and are not allowed.)

There are only three linear homogeneous equations (in a, b, c) to be solved. That is because the potentials, unlike the hopping terms, fall off quickly with distance. Had we kept next-nearest-neighbor interactions, the numerator in Eq. (18) would be augmented by $b' \cos 2k_x + c' \cos 2k_y$ and there would be five equations in the five unknowns. Our calculations show that coefficients of the extra terms in b' and c' are considerably smaller than those of b and c and are legitimately discarded.

A solution of the 3×3 matrix requires the vanishing of a secular determinant with two distinct roots. The first yields

$$1 + 2[\mathbf{V}(x) - \mathbf{J}(x)] T^2(1,0) [G_2 - G_3] = 0, \quad (19)$$

and corresponds to a d -wave solution, while the second, s -wave, solution yields

$$\begin{aligned} & 1 + 2[\mathbf{V}(x) - \mathbf{J}(x)] T^2(1,0) [G_2 + G_3] \\ & + \mathbf{u}(x) \{G_0 + 2[\mathbf{V}(x) - \mathbf{J}(x)] T^2(1,0) \\ & \times [G_0(G_2 + G_3) - 2G_1^2]\} = 0. \end{aligned} \quad (20)$$

Here the G 's are

$$G_0(x|E) = \frac{1}{N} \sum_{k \in \text{BZ}} \frac{1}{2\varepsilon(k) + |E|},$$

$$G_1(x|E) = \frac{1}{N} \sum_{k \in \text{BZ}} \frac{\cos k_x}{2\varepsilon(k) + |E|},$$

$$G_2(x|E) = \frac{1}{N} \sum_{k \in \text{BZ}} \frac{\cos^2 k_x}{2\varepsilon(k) + |E|}$$

and

$$G_3(x|E) = \frac{1}{N} \sum_{k \in \text{BZ}} \frac{\cos k_x \cos k_y}{2\varepsilon(k) + |E|}.$$

In general, Eq. (19) has no solution for $x < x_c$ and similarly for Eq. (20). We have calculated the above integrals for the p -type materials and used them to estimate x_c . Our calculations yield minimum values $x_c = 6.913$ for s pairing in Eq. (20) and $x_c \approx 9$ for d pairing in Eq. (19). Although the s -pairing solution sets in earlier and is clearly more stable than the d -pairing solution, neither type solution exists within the physically reasonable range, $0 < x < 3.8$. To extend the analysis to a finite density of charge carriers we next turn to the self-consistent BCS equations.¹¹

XIII. CRITICAL TEMPERATURE AND THE GAP

We start from the equation for the energy gap at temperature T ,

$$\Delta_p = -\frac{1}{N} \sum_k \hat{V}_{p,k} \frac{\Delta_k}{2E_k} \tanh(\frac{1}{2} \beta E_k),$$

$$\Delta_p = a + b \cos p_x + c \cos p_y, \quad (21)$$

in which all the potentials are included in $\hat{V}_{p,k}$, $\beta = 1/k_B T$, $E_k = \sqrt{\varepsilon_k^2 + \Delta_k^2}$, and $\varepsilon_k \equiv \varepsilon(k) - \mu$ is the energy measured from a Fermi level μ within the band. Once again there are two types of solutions: the s wave with $a \neq 0$ and $b = c$, and the d wave with $a = 0$ and $c = -b$. At T_c the gap vanishes and the secular determinant decouples into two equations identical to Eqs. (19) and (20). Only the definition of the Green functions has been changed.²⁶ They are now functions of x , T_c and μ :

$$G_0(\beta_c | \mu) = \frac{1}{N} \sum_{k \in \text{BZ}} \frac{1}{2\varepsilon_k} \tanh \frac{1}{2} \beta_c \varepsilon_k,$$

$$G_1(\beta_c | \mu) = \frac{1}{N} \sum_{k \in \text{BZ}} \frac{\cos k_x}{2\varepsilon_k} \tanh \frac{1}{2} \beta_c \varepsilon_k,$$

$$G_2(\beta_c | \mu) = \frac{1}{N} \sum_{k \in \text{BZ}} \frac{\cos^2 k_x}{2\varepsilon_k} \tanh \frac{1}{2} \beta_c \varepsilon_k,$$

and

$$G_3(\beta_c | \mu) = \frac{1}{N} \sum_{k \in \text{BZ}} \frac{\cos k_x \cos k_y}{2\varepsilon_k} \tanh \frac{1}{2} \beta_c \varepsilon_k. \quad (22)$$

We solve each equation numerically for $T_c(\mu)$. As might be expected from the preceding two-particle calculation, in the p -type materials there are no solutions of either symmetry for μ near the bottom of the band, for any physically reasonable value of x . However, as μ is increased, we start to find an s -paired solution (corresponding to mediocre values of T_c) for μ ranging from 1/5 to 1/2 [we are using convenient dimensionless units, in which the energy of the van Hove singularity is $\omega(k) = 1$; cf. Figs. 1 and 2]. This solution disappears beyond $\mu = 0.5$, owing to a factor $(\cos k_x + \cos k_y)^2$ in the integrand which multiplies the density of states. This is the relevant structure factor for s pairing in this lattice. It vanishes at the van Hove singularity and effectively quenches s pairing at midband, while the low density of states at the bottom of the band has the same effect. Consequently, we look to the d -pairing solution for an explanation of high- T_c superconductivity.

For $\mu > 0.7$ we find only the d -paired solutions. Here the corresponding factor in the integrand is essentially $(\cos k_x - \cos k_y)^2$, which is also small at the band edges but finite near the singularity. In our calculations, the d -paired solutions yield values of T_c which rise slowly but monotonically with increasing Fermi energy, to a maximum as $\mu \rightarrow 1$.²⁷

In Fig. 7 we plot T_c for d pairing, as function of x , at $\mu = 0.85$. This corresponds to a filling factor ν of some 90%, sufficiently far from the antiferromagnetic phase boundary to ensure that the results are not spurious. We find the $T=0$ gap parameter b by solving Eq. (19) using the Green functions,

$$G_2(b | \mu) = \frac{1}{N} \sum_{k \in \text{BZ}} \frac{\cos^2 k_x}{2E_k}$$

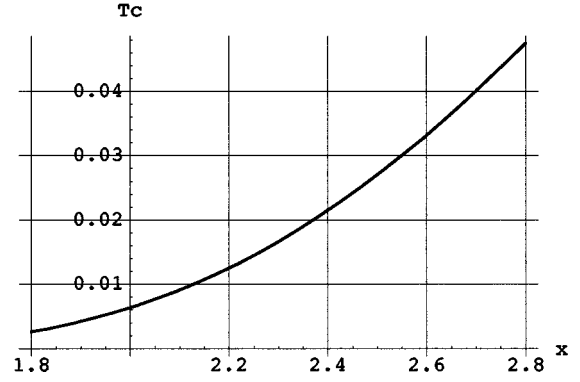


FIG. 7. $kT_c(x)$ in units of t^* , as obtained from the d -pair solution of the BCS equation, Eq. (21), at filling factor $\nu = 0.9$.

and

$$G_3(b | \mu) = \frac{1}{N} \sum_{k \in \text{BZ}} \frac{\cos k_x \cos k_y}{2E_k}, \quad (23)$$

where

$$E_k = \sqrt{\varepsilon_k^2 + b^2 (\cos k_x - \cos k_y)^2}.$$

At the few points where we checked, b was approximately $3/2T_c$, although in general the ratio of this gap parameter to T_c appears to be a function of μ .

CONCLUSION AND FUTURE PLANS

With experimental knowledge of such quantities as T_c , b , J , W_{eff} , etc., it should be possible to determine t^* and x unambiguously for a given copper-oxide material. We are in the process of making this fit.

Despite initial skepticism, the existence of d pairing high- T_c superconductivity in copper-oxide materials has by now been confirmed in innumerable experiments. The present calculations favor it unambiguously at midband (but not at the band edges) over the more conventional s pairing, primarily as a consequence of the nearest-neighbor structure factor. In future work we shall revisit the model near the antiferromagnetic phase boundary, with the aid of appropriate many-body methods. We have examined interference of the higher-order multisite hopping terms with the leading-order hopping terms, to the extent that this affects the band structure of the composites and report on this elsewhere. Finally, we intend to reexamine the various simplifying assumptions underlying the present work.

Our principal result, presented in this paper, consists in the demonstration that the properties of the low-lying states of the $3N$ orbitals in a copper-oxide plane are faithfully represented by just N composite states of a single-band model and their many interactions, as summarized in Eq. (14). We showed that it is possible for large numbers of physically important quantities, hopping parameters and interaction potentials, to be linked by a few parameters—just two in our simplified model: one being nontrivial parameter x , and the other, just unit of energy t^* .

- ¹Originally based on orthogonal orbitals, the limit model yielded at first only repulsive zero-range interactions and thus no plausible explanation for high- T_c superconductivity. With the introduction of nonorthogonal orbitals it proved possible to extract an attractive superexchange interaction, albeit of undetermined strength. The original studies are in D. C. Mattis, Phys. Rev. Lett. **74**, 3676 (1995); Mod. Phys. Lett. B **8**, 1387 (1994). Optical absorption within this model was analyzed in D. C. Mattis and J. M. Wheatley, *ibid.* **9**, 1107 (1995). Nonorthogonal orbitals were introduced into the limit model by D. C. Mattis and J. M. Wheatley, Phys. Rev. B **52**, 15 103 (1995).
- ²The variety of three-band models includes H. Eskes *et al.*, Physica C **160**, 424 (1989); M. S. Hybertsen *et al.*, Phys. Rev. B **41**, 11 068 (1990); L. F. Feiner *et al.*, *ibid.* **53**, 8751 (1996); R. Eder, Y. Ohta, and G. A. Sawatzky, *ibid.* **55**, R3414 (1997) *inter alia*. Earlier works include A. Fujimori and F. Minami, *ibid.* **30**, 957 (1984); G. A. Sawatzky and J. W. Allen, Phys. Rev. Lett. **53**, 2339 (1984); J. Zaanen, G. A. Sawatzky, and J. W. Allen, *ibid.* **55**, 418 (1985); A. Fujimori, Phys. Rev. B **39**, 793 (1989); F. Mila, *ibid.* **38**, 11 358 (1988); A. K. McMahan, R. M. Martin, and S. Satpathy, *ibid.* **38**, 6650 (1988); H. Eskes, L. H. Tjeng, and G. A. Sawatzky, *ibid.* **41**, 288 (1990). All differ in approach and detail from one another and from the present work.
- ³We estimate x to be close to the upper limit in the range $0.5 < x < 3$ for the known copper-oxide-based materials.
- ⁴A thorough review of recent work on standard (and variant) Hubbard and t - J models is given by E. Dagotto, Rev. Mod. Phys. **66**, 763 (1994).
- ⁵“Band” is actually a misnomer, as models based on atomic orbitals and incorporating two-body correlations are unrelated to familiar one-electron band-structure calculations. The latter are found to have shortcomings in CuO [see J. Ghijsen *et al.*, Phys. Rev. B **38**, 11 322 (1988)], and thus, *a fortiori*, in CuO₂, owing to the neglect of dynamic correlations. Attempts to rectify these shortcomings have had some limited success, e.g., the “slave boson” band-structure approach for Y-Ba-Cu-O by M. Biagini, Phys. Rev. Lett. **77**, 4066 (1996) identifies a van Hove singularity 25 meV below the Fermi level in qualitative accord with the photoemission spectrum, which locates it some 19 meV below the Fermi level, e.g., K. Gofron *et al.*, *ibid.* **73**, 3302 (1994). However, a number of authors have ascribed this “extended van Hove singularity” to the many-body correlations. See N. Bulut *et al.*, *ibid.* **72**, 705 (1994); E. Dagotto *et al.*, *ibid.* **73**, 728 (1994); and most recently W.-G. Yin, C.-D. Gong, and P. W. Leung, *ibid.* **81**, 2534 (1998). If they are correct, this phenomenon would be only remotely related to the spectrum of one-particle Bloch energies. Last but not least, there is disagreement whether this singularity is even a feature which is shared by *all* copper-oxide-based high- T_c materials, or whether it is an accidental, and therefore less interesting, property of some of them; see S. LaRosa *et al.*, Phys. Rev. B **56**, R525 (1997).
- ⁶J. Hubbard, Proc. R. Soc. London, Ser. A **277**, 237 (1964); the modifications to accommodate two species of ions are along the lines proposed some time ago by V. Emery, Phys. Rev. Lett. **58**, 2794 (1987); P. W. Anderson, Science **235**, 1196 (1987).
- ⁷The interaction of two extra electrons in an oxygen $2p$ orbital *has to be* weak, since these ions are known to accommodate valences 2, 1, and 0 with equal ease whenever the chemical potential is positioned near the energy of the singly occupied $2p$ orbital.
- ⁸According to the Pauli principle they have, perforce, opposite spins.
- ⁹H. Takagi, Y. Tokura, and S. Uchida, Physica C **162-164**, 1101 (1989); S. Uchida, H. Takagi, and Y. Tokura, *ibid.* **162-164**, 1677 (1989).
- ¹⁰The antiferromagnetic phase of the copper oxides has been intensely analyzed by a variety of theoretical and numerical many-body techniques and fitted to experiment in such papers as B. Keimer *et al.*, Phys. Rev. B **46**, 14 034 (1992); see the most recent review by M. A. Kastner, R. J. Birgeneau, G. Shirane, and Y. Endoh, Rev. Mod. Phys. **70**, 897 (1998). In the present paper, we are concerned mainly with the metallic and/or superconducting phase, and make no attempt to examine the antiferromagnetic insulating phase which, experimentally, is only stable at or near $\nu=1$, i.e., five electrons *per* cell.
- ¹¹Here we follow J. R. Schrieffer, *Theory of Superconductivity* (Benjamin, New York, 1964), Chap. 2.
- ¹²While the present theory is developed for both p - and n -type materials, the actual calculations in the text are all for the former, given their greater utility. However, the interested reader can easily obtain similar results for the latter or can request them from the author.
- ¹³However, for completeness, all states *including* the high-energy states are required in the perturbation theory.
- ¹⁴F. C. Zhang and T. M. Rice, Phys. Rev. B **37**, 3759 (1988).
- ¹⁵Taking away an electron from the i th cell and putting the cell into the $|3\sigma, i\rangle$ configuration would yield $q_i = +1$ at a cost of energy $E_3 - E_4$ which is the same as $E_5 - E_4$. However, because it is energetically cheaper to remove a zero-energy electron from the filled β band, the $|3\sigma, i\rangle$ are not automatically accessed if we just specify $q_i = +1$ and thus do not play the same important role in the model as do the $|5\sigma, i\rangle$ for $q_i = -1$. (They do play a role as virtual states accessed in the perturbation theory.)
- ¹⁶The remaining ten matrix elements connect the initial state to states of higher energy and thus, to leading order, enter only in the self-energy of the $q = -1$ cell.
- ¹⁷E.g., M. W. Long and X. Zotos, Phys. Rev. B **48**, 317 (1993).
- ¹⁸By a property of second-order perturbation theory, it is, in fact, a *lower* bound to the exact ground-state energy of the model.
- ¹⁹Some experimental observations have identified an “extended van Hove singularity” some 10–30 meV *below* the Fermi level rather than lying above it: K. Gofron *et al.*, J. Phys. Chem. Solids **54**, 1193 (1993); Phys. Rev. Lett. **73**, 3302 (1994) in Y-B-Cu-O; D. S. Dessau *et al.*, *ibid.* **71**, 2781 (1993); D. M. King *et al.*, *ibid.* **73**, 3298 (1994) in Bi-Sr-Ca-Cu-O; and T. Yokoya *et al.*, *ibid.* **76**, 3009 (1996) in the noncuprate Sr₂RuO₄, p -type materials. While this may appear to contradict the spectrum illustrated in Figs. 1 and 2 of the present work, we note that some published computer simulations, molecular dynamics, and/or exact diagonalization studies on small clusters, based on simple t - t' - J models do fit these observations and ascribe shifts in the positions of the singularities to the dynamics of the strongly interacting particles; see discussion in Ref. 5.
- ²⁰Because of the difference in signs, the motional energy of 5's in a background of 6's has its minimum at $k=0$. Expansion about $k=0$ yields $\Delta E_5(k) = \text{const} + k^2/2M$, which in two dimensions yields an unexceptional, constant, density-of-states near the band edge.
- ²¹In the spirit of the Born-Oppenheimer approximation we fix the particles at the specified sites for the purpose of calculating their interactions.

- ²²However, if two $5\uparrow$'s are introduced into the sea of 6 's the total excitation energy $\Delta E_{\uparrow\uparrow}$ does not depend on their separation and the scalar potential vanishes: $V_{55,6}(R)=0$, at all x .
- ²³ $V(R)$ was believed to vanish in the limit model, Ref. 1, because the last term in [] in Eq. (12a) does not even *appear* at $x=0$. However, now we are calculating at finite x , retaining all the terms and then proceeding to the limit $x\rightarrow 0$ and by l'Hopital's rule this term is nonzero—indeed, maximal—in the limit $x\rightarrow 0$, although it is never large nor even comparable to U_{eff} .
- ²⁴C. Y. Chen *et al.*, Phys. Rev. B **43**, 1 (1991).
- ²⁵E.g., A. E. Ruckenstein, P. J. Hirschfeld, and J. Appel, Phys. Rev. B **36**, 857 (1987).
- ²⁶Although the BCS equations are identical to those for the two-body bound state, now the interactions are no longer being treated precisely, but in what has been termed a generalized Hartree-Fock approximation. Both they, and the energies ε_k , should be renormalized. At higher densities, the antiferromagnetic correlations should be taken into account. Finally, fluctuations play a non-negligible role in two dimensions. These important considerations are all beyond the scope of the present work but will be addressed elsewhere.
- ²⁷Of course, these solutions do not take into account the increasing competition with antiferromagnetic correlations as the boundary to the antiferromagnetic phase is approached. The observed *drop* in T_c from its maximum near $\nu=0.85$ to $T_c=0$ at the magnetic phase boundary should also flow from a comprehensive theory.